S.C. Forth [1], J.C. Newman, Jr. [2], and R.G. Forman [3]

Evaluation of Fatigue Crack Thresholds Using Various Experimental Methods

REFERENCE: Forth, S. C., Newman, Jr., J.C. and Forman, R.G., "**Evaluation of Fatigue Crack Thresholds Using Various Experimental Methods**," ***Fatigue and Fracture Mechanics: 34th Volume, ASTM STP 1461,*** S. R. Daniewicz, J. C. Newman, Jr., and K. H. Schwalbe, Eds., ASTM International, West Conshohocken, PA, 2004.

ABSTRACT: The accurate representation of fatigue crack threshold, the region defining crack growth as either very slow or nonexistent, is extremely important. If the experimentally measured threshold is unconservatively high, a structural component designed with this data may fail long before the fatigue analysis predicts. The fatigue crack growth threshold is experimentally defined using ASTM standard E647, which has been shown to exhibit anomalies. Alternate test methods have been proposed, such as the constant K_{max} test procedure, to define the threshold regime without ambiguity. However, only the current test method defined by ASTM is designed to produce the range of fatigue crack thresholds (*e.g.* low and high *R*) needed to characterize an aerospace loading environment. It is the scope of this paper to determine the fatigue crack growth threshold of a well characterized aerospace alloy, 7075-T7351 aluminum, using different methods, compare the results, and draw conclusions.

KEYWORDS: fatigue, threshold, crack growth, test methods, plasticity induced crack closure.

Introduction

Fatigue crack growth in a material is typically quantified by the size of the crack, *a*, and the rate at which it propagates, *da/dN*. The crack growth rate through a given material is expressed as a function of the linear-elastic fracture mechanics term, ΔK, the stress intensity factor range. This relationship was originally shown to be linear over a large range of fatigue crack growth rates on a log-log scale [1]. However, the relation between crack growth rate and stress intensity is nonlinear when the cracked body is approaching fracture [2], and when the crack growth rate is very slow [3]. Therefore, the three idealized regions of crack growth are defined as the threshold region (slow growth), the linear region (stable growth) and the fracture region (rapid growth) illustrated in FIG 1.

Ideally, the fatigue crack growth threshold is the asymptotic value of ΔK at which *da/dN* approaches zero [4]. Currently, the threshold is used as a limit for damage tolerant design [5], *e.g.* if the stress intensity factor for a given crack is below the threshold value, the crack is assumed to be nonpropagating [6]. However, it has been shown that small cracks propagate at ΔK below the threshold value [7] defined using the ASTM standard

[1] Research Engineer, NASA Langley Research Center, 2 West Reid Street, Mail Stop 188E, Hampton, VA 23681
[2] Professor, Department of Aerospace Engineering, 330 Walker Engineering Lab., Hardy Street, Mississippi State University, Mississippi State, MS 39762
[3] Senior Scientist, NASA Johnson Space Center, 2101 NASA Road 1, Mail Code EM2, Houston, TX 77058

test procedure. This small crack work studied the growth of microstructural defects [8] inherent to the material [9] that propagate to failure before the design life is reached. Therefore, if the fatigue crack growth threshold is to be established as a lifing criterion, then the most accurate representation of the fatigue characteristics of a material need to be defined.

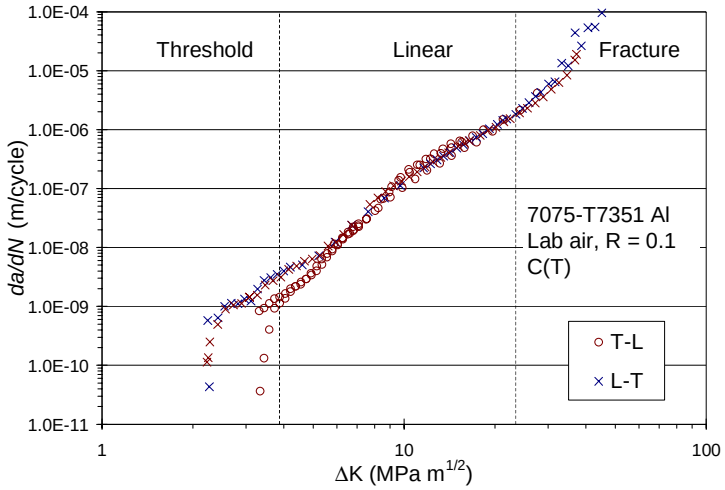

FIG 1— *Definition of crack growth regions for T-L and L-T data at R = 0.1.*

The ASTM standard E647 defines an experimental procedure to operationally determine fatigue crack growth threshold. This standard recommends that the threshold stress intensity factor range correspond to a crack growth rate of 10^{-10} m/cycle, which is also used for this study. The specifications for achieving this rate are outlined in the standard using either constant *R* or constant K_{max} load reduction methods, graphically depicted in FIG. 2. The constant *R* load reduction method reduces the maximum and minimum load applied to a cracked specimen such that the load ratio, *R* ($R = K_{min}/K_{max} = P_{min}/P_{max}$) remains constant. The constant K_{max} test procedure imposes a constant K_{max} [10, 11] while increasing K_{min} [12, 13]. However, for tensile loading, the constant K_{max} test procedure is constrained to producing high *R* data at threshold. This has been an artifact of the specimen configuration; pin loaded C(T) specimens (similar to the GC(T) specimen in FIG. 3) cannot be subjected to high compressive stresses due to the geometric instability of pin loaded specimens. Hence, to achieve a constant K_{max} threshold for low and negative *R* values, the middle-crack tension, M(T), specimen (FIG. 4) was employed, which can be tested at high compressive loads [14].

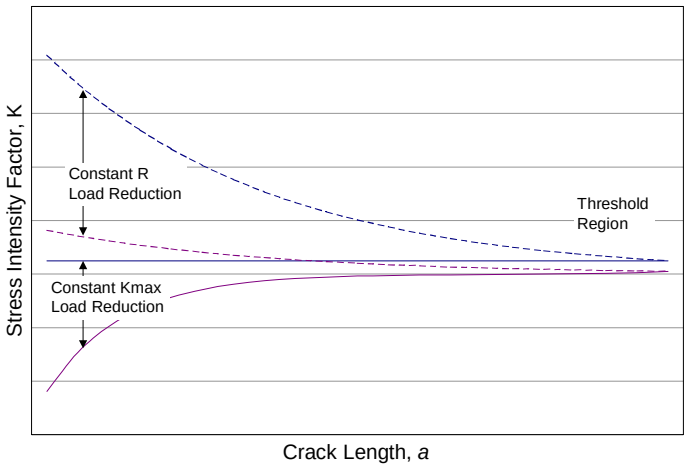

FIG. 2— *Schematic of load reduction methods (Constant R and Constant K_{max}).*

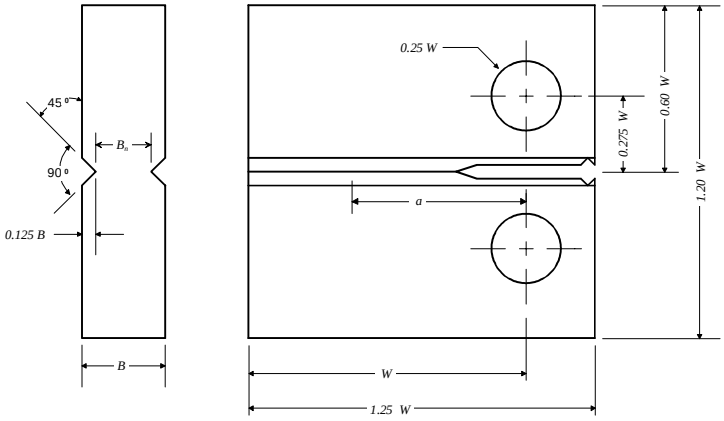

FIG. 3— *Schematic of side-grooved compact tension specimen, GC(T) (W = 76.2 mm, B = 12.7 mm, B_N = 9.53 mm, initial notch length (a) of 19.1 mm).*

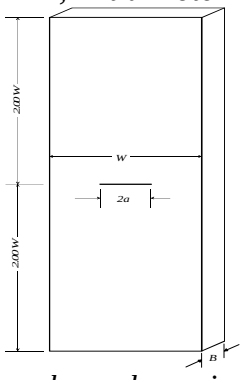

FIG. 4— *Schematic of middle through crack specimen, M(T). (W = 76.2 mm, B = 12.7 mm, initial notch width (2a) of 12.7 mm).*

Experimental results suggest that the constant *R* load reduction test procedure develops remote plasticity-induced crack closure [15, 16] that can lead to elevated threshold data. The amount of crack-wake plastic deformation produced during a test is directly related to the magnitude of previously applied crack tip loads, *i.e.* higher K, more plasticity [17]. The constant *R* load reduction test starts at a high load, and sheds load

until threshold is reached. Therefore, the initial K will produce larger plastic deformations than subsequent conditions. This plastic wake, or history, can affect the crack driving mechanisms, *i.e.* during the unloading process the crack will close first at some point along the wake, reducing the effective load at the crack tip [18, 19]. This remote closure concept is graphically depicted in FIG. 5. Additionally, the compact tension specimen traditionally used to generate fatigue crack growth data, utilizes a notch to initiate crack growth. A crack emanating from a notch often exhibits plane stress behavior near the notch root [20] (FIG. 6), and transitions to a combination of plane strain/stress as the notch effect diminishes. Plane strain plasticity is approximately one-third the size of plane stress [21] further enhancing any plasticity effects at the notch root. Cracks propagating in a material exhibit plane strain behavior in the interior and plane stress behavior at the surface [22], as depicted in FIG. 7, leading to a higher probability of the surface closing prior to the interior. Therefore, if fatigue crack growth data is to be generated with minimal plasticity history effects, so as not to affect test data, then a modification of the specimen geometry and/or test procedure should be made.

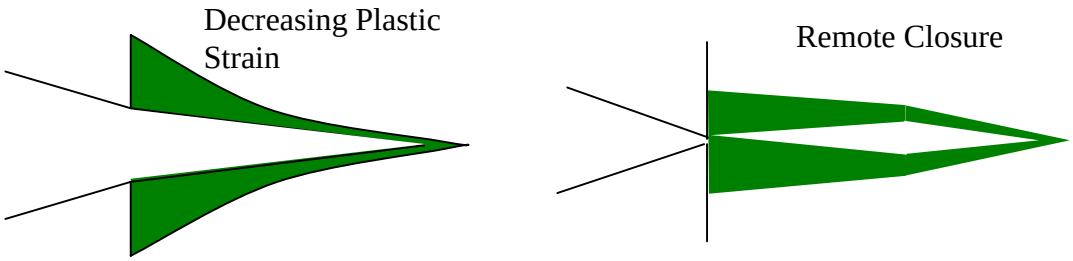

FIG. 5— *Graphical depiction of remote closure.*

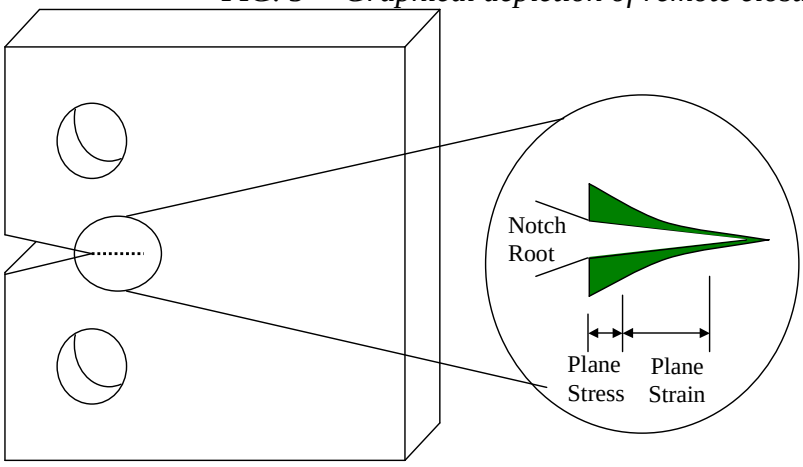

FIG. 6— *Plane stress plastic zone at the notch root.*

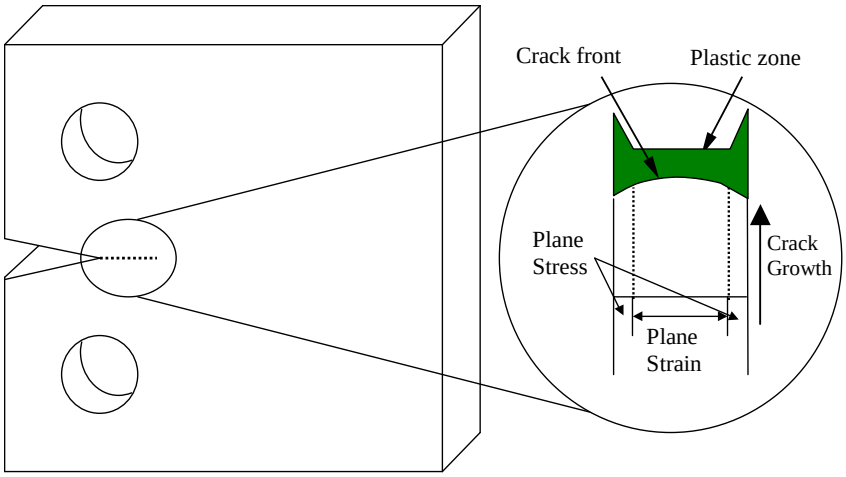

FIG. 7— *Plastic zone in front of the crack.*

Modification of the C(T) specimen geometry to include side-grooves, GC(T), was implemented to force the crack to maintain plane strain behavior by achieving a nearly constant tri-axial stress state along the crack front [23]. The plane strain conditions are realized by removing the material exhibiting plane-stress behavior at the surface, approximately 25% of the specimen thickness, by introducing 45^{o} grooves along the edges (FIG. 3). As a result, the plastic strains generated along the specimen surface will be as low as one third that of a full thickness specimen [24].

One way to reduce the effect of remote crack closure is to produce a crack with a larger plastic zone size at the crack tip than along any point in the wake. This can be accomplished by plastically compressing the crack wake [25]. Hence, if compressive loads are used for precracking, the plane stress plastic wake at the notch will be minimal, and not influence the subsequent test results [26]. Another solution to remote closure is to produce fatigue crack growth data by constantly increasing the K under constant amplitude loading conditions [27, 28]. The test will impart a constantly increasing plastic zone such that the plastic wake will never close prior to the crack tip closing. Ideally, an increasing K methodology will produce results with little plastic history as steady-state is achieved; there are few plastic wake effects to instigate remote closure; and a "history-free" crack growth curve can be generated using one specimen. In this paper, the authors present fatigue crack growth threshold test data using constant *R* and constant K_{max} load reduction and K increasing test procedures, employing both standard and side-grooved compact tension specimens, and constant K_{max} tests with compression-compression precracking.

Experimental Methods

The constant *R* load reduction method, prescribed by ASTM E647, generates quasi-steady-state fatigue crack growth rates into the threshold region. The generation of near-threshold data is accomplished by reducing the applied load on the specimen in a controlled manner such that the load ratio, *R*, is kept constant, *e.g.* the maximum and minimum load are continuously reduced throughout the test. The constant K_{max} load reduction method also reduces both the maximum and minimum load to generate threshold data, however the value of K_{max} is constant, *i.e. R* is varying. Controlling the test via stress intensity factors is achieved through monitoring of the crack length during

testing and adjusting loads. For the constant K_{max} load reduction test procedure, the applied loads are varied to maintain a constant K_{max} value while increasing (the absolute value of) K_{min} until the rate of crack growth reaches a predefined amount, in this case the ASTM specified 10^{-10} m/cycle. The rate of load shedding for both procedures is defined by the equation

$$C = \left(\frac{1}{K}\right)\left(\frac{\Delta K}{da}\right) \tag{1}$$

where C is the normalized K gradient and for the case of a compact tension, C(T), specimen, the stress intensity factors are defined as

$$\Delta K = \frac{\Delta P}{\beta\sqrt{W}} \frac{(2+\alpha)}{(1-\alpha)^{3/2}} \left(0.886 + 4.64\alpha - 13.32\alpha^2 + 14.72\alpha^3 - 5.6\alpha^4\right) \tag{2}$$

where

$$\beta = \begin{cases} \mathrm{B} & \mathrm{C(T)\ specimens} \\ \sqrt{\mathrm{B}\cdot\mathrm{B_N}} & \mathrm{GC(T)\ specimens} \end{cases} \text{ [29],}$$

$\alpha = a/W$ for $a/W \geq 0.2$ [30],

ΔP is the applied load range, W is the width of the specimen, B is the thickness of the specimen, B_N is the thickness of the specimen between the side-grooves, and a is the crack length. For this study, the dimensions of the C(T) and GC(T) specimens are defined in FIG. 3, where W = 76.2 mm, B = 12.7 mm, B_N = 9.53 mm (GC(T) only) and an initial notch length of 19.1 mm. The stress intensity solution for an M(T) specimen is given as

$$\Delta K = \frac{\Delta P}{B}\sqrt{\frac{\pi\alpha}{2W}\sec\frac{\pi\alpha}{2}} \tag{3}$$

where

$\alpha = 2a/W$ for $2a/W < 0.95$ [31],

B is the specimen thickness and W is the width. For this study, M(T) dimensions are defined in FIG. 4, where W = 76.2 mm, B = 12.7 mm and the initial notch is 12.7 mm.

The normalized K gradient, C, is algebraically limited to a value greater than –80 meter^{-1} [32, 33], which ensures the rate of load shedding to be gradual enough to "1) preclude anomalous data resulting from reductions in the stress-intensity factor and concomitant transient growth rates, and 2) allow the establishment of about five *da/dN*, ΔK data points of approximately equal spacing per decade of crack growth rate", as per section 8.6.2 of the ASTM standard E647. FIG. 2 graphically depicts the constant R and constant K_{max} load reduction methods.

The compact tension, C(T), and grooved compact tension specimens, GC(T), were precracked with a constant ΔK that is equivalent to the first data point in the load reduction test, unless otherwise noted. These loads were applied until the crack length was an *a/W* of 0.3, as per the ASTM standard. The M(T) tests were precracked using a high compression scheme based on the closure-free test procedures proposed by Au, *et al.*, [34]. The precracking loads, both maximum and minimum loads in compression, were applied until the crack growth rate, *da/dN*, was less than 10^{-10} m/cycle. This compressive scheme was used to produce an initial flaw that had little plastic history [35], so as not to affect the subsequent test [36].

The K increasing test procedure was developed to produce fatigue crack growth data with minimal plastic history effects [27, 28]. This was accomplished by first producing a crack from a notch using compressive precracking loads. Then the crack was propagated using a small tensile load, such that the stress intensity factor range was approximately 0.5 MPa $m^{1/2}$, to grow out of the residual tensile stress field developed by the compressive loading [36]. Then, constant amplitude loading was applied at a specific *R* value to generate a fatigue crack growth rate curve, *i.e.* as the crack propagates, K increases as does *da/dN*. The applied load was computed based on prior knowledge of the threshold stress intensity factor and the measured crack length. If the crack growth rate was less than 10^{-10} m/cycle, the applied load was increased by 10%, and this was continued until the measured crack growth rate exceeded 10^{-10} m/cycle. The remaining data would then be generated at this load level.

Fatigue Crack Growth Rate Data

The constant *R* and constant K_{max} load reduction tests were conducted using a software-control system on an servo-hydraulic machine with a clip gage to measure compliance and determine crack length, in lab air at a mean temperature of 21^{o} C. The compliance crack length measurements were calibrated visually with a floating microscope. The K_{max} tests conducted using the M(T) specimens were produced under constant load amplitude conditions and the crack lengths were measured visually on both front and back surfaces using floating microscopes. These tests were also conducted in lab air at a mean temperature of 21^{o} C.

The majority of the constant *R* load reduction tests were performed in the T-L grain orientation as the primary loading direction. Whereas, the M(T) and GC(T) specimens were orientated such that the L-T grain direction was the primary loading direction. There is evidence in the literature that the grain orientation can have an effect on the fatigue crack growth properties of this aluminum alloy [37]. Therefore, a series of constant *R* load reduction tests were performed in the L-T direction to compare the effect of grain orientation on the fatigue crack growth rate. As shown in FIG 1, the difference between the two orientations is most pronounced at threshold. Therefore, all plots that contain L-T and T-L data will be marked accordingly. The constant *R* load reduction tests were precracked at a constant ΔK that is equivalent to the first data point in the load reduction test, unless otherwise noted.

The M(T) K_{max} tests were conducted using a high compression scheme for precracking, such that the maximum applied load was –6.79 MPa and the minimum was –207 MPa at a notch width of 12.7 mm. The first test was run at a constant K_{max} of 1.65 MPa $m^{1/2}$ to achieve a threshold of 1.86 MPa $m^{1/2}$ at $R = -0.13$. The second test was run at a constant K_{max} of 2.20 MPa $m^{1/2}$ to produce a threshold of 0.95 MPa $m^{1/2}$ at an *R* of 0.57. The third K_{max} test was run at a K_{max} value of 1.65 MPa $m^{1/2}$ producing a threshold of 1.65 MPa $m^{1/2}$ at an *R* of 0.00. Note that the first and third tests were conducted at the same K_{max} level and load reduction rate yet produced different threshold values at different *R*. The data produced from the constant K_{max} load reduction tests is shown in FIG. 8. Once the threshold rate was achieved (10^{-10} m/cycle), a K increasing test was run corresponding to the *R* value at threshold. These results are plotted in FIG. 9.

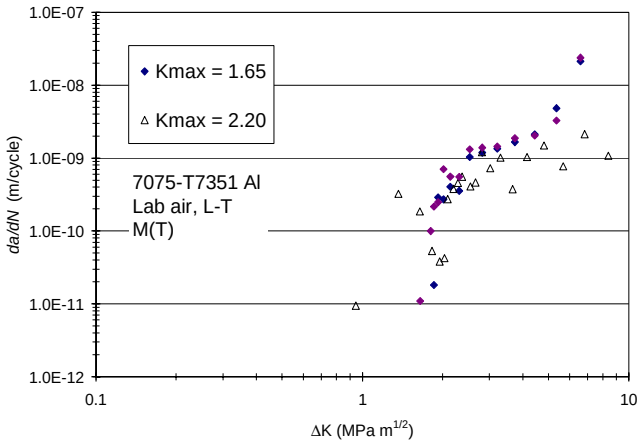

FIG. 8— *Constant K_{max} load reduction data.*

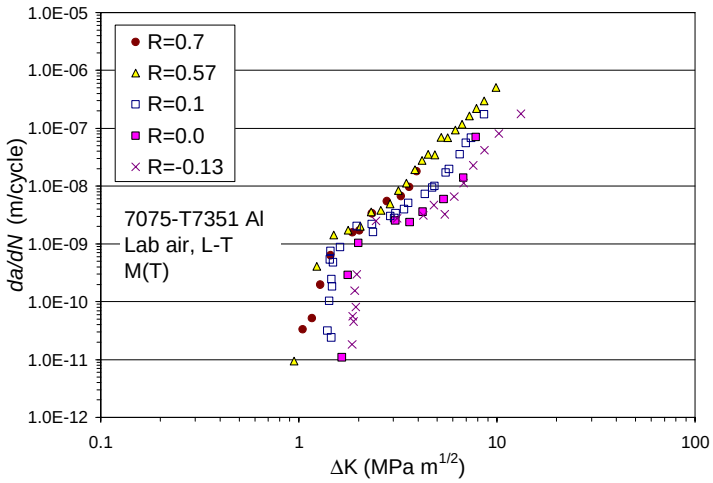

FIG. 9— *K increasing data.*

Data was generated for the R = 0.1 condition because closure was expected at this stress ratio. The data shown in FIG. 10 was generated using constant R load reduction, with standard tensile precracking loads on both standard C(T) and GC(T). The constant R load reduction tests using standard precracking methods on a C(T) yielded a threshold of 2.30 MPa $m^{1/2}$. Using the same load reduction technique on a GC(T) specimen yielded a threshold of 1.37 MPa $m^{1/2}$. The crack growth curves generated using the GC(T) specimens experience a "bounce" at $\Delta K \sim 1.9$ MPa $m^{1/2}$ (*i.e.* the crack growth rate decreased with decreasing ΔK, then increased with decreasing ΔK, then decreased with decreasing ΔK). This phenomenon is discussed in further detail in the following section. The compression-compression precracking, K increasing scheme used with a GC(T) produced a threshold of 1.46 MPa $m^{1/2}$ without exhibiting this bounce effect. M(T) and C(T) specimens were also run with compression-compression precracking and a K increasing scheme at constant R, and exhibited a threshold value of 1.45 MPa $m^{1/2}$ (M(T)) and 1.49 MPa $m^{1/2}$ (C(T)) respectively. This data is shown in FIG. 11 for the L-T grain orientation, omitting the GC(T) tensile precracking data. A comparison of the K increasing and K decreasing data for the C(T) specimen is shown in FIG. 12. The threshold values are summarized in Table 1.

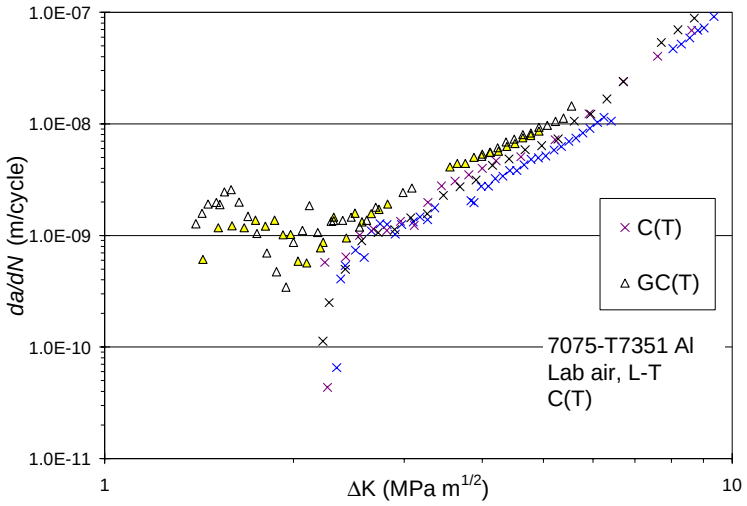

FIG. 10— *R = 0.1 da/dN vs. ΔK data.*

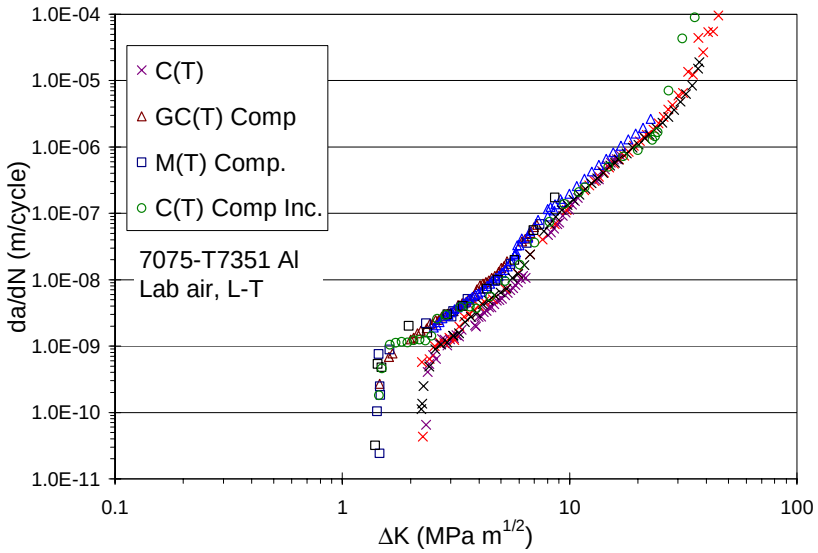

FIG. 11— *R = 0.1 da/dN vs. ΔK data.*

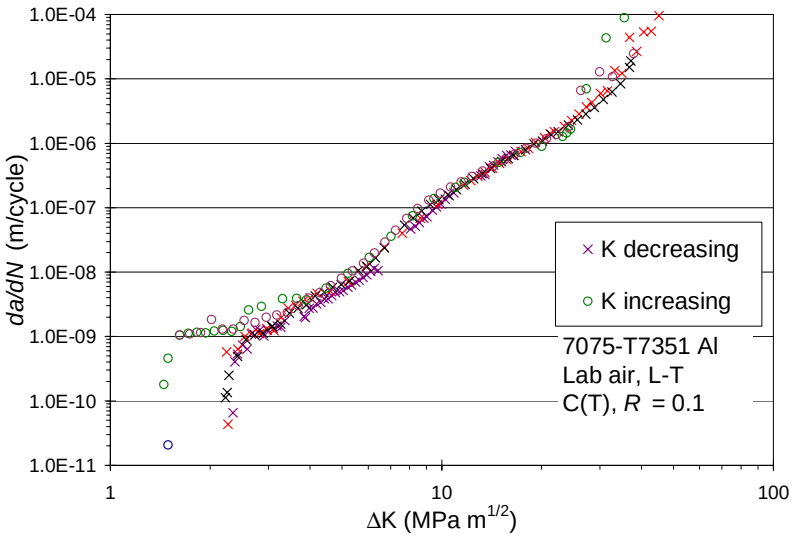

FIG. 12— *Comparison of K increasing and K decreasing test data.*

Data was also generated for the $R = 0.7$ condition to examine a stress level where closure was not expected. The data shown in FIG. 13 was generated using constant R load reduction, with tensile precracking loads on both C(T)s and GC(T)s. M(T) specimens were run with compression-compression precracking and a K increasing scheme at constant amplitude. The constant $R = 0.7$ load reduction tests using standard precracking methods on a C(T) yielded a threshold of 1.23 MPa $m^{1/2}$. Using the same load reduction technique on a GC(T) specimen yielded a threshold of 1.12 MPa $m^{1/2}$. The M(T) test, an increasing K test under constant amplitude loading, exhibited a threshold value of 1.05 MPa $m^{1/2}$. The threshold values are summarized in Table 1.

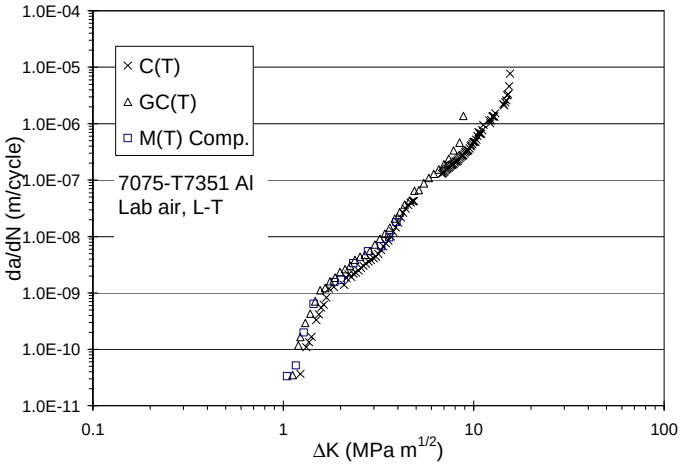

FIG. 13— *R = 0.7 da/dN vs. ΔK data.*

Fatigue crack growth threshold data generated in the T-L grain orientation is plotted in FIG. 14. All of the tests were conducted using the constant R load reduction procedure on C(T) specimens, with a precracking load equal to the initial data point. Threshold data was generated for R of 0.1, 0.4, 0.7, 0.8 and 0.9 with values of 3.34, 2.09, 1.27, 1.27 and 1.05 MPa $m^{1/2}$, respectively. These curves are plotted separately due to the lack of

comparative data (*i.e.* same T-L orientation) using other test procedures. However, this data is valuable baseline data for comparison of future testing.

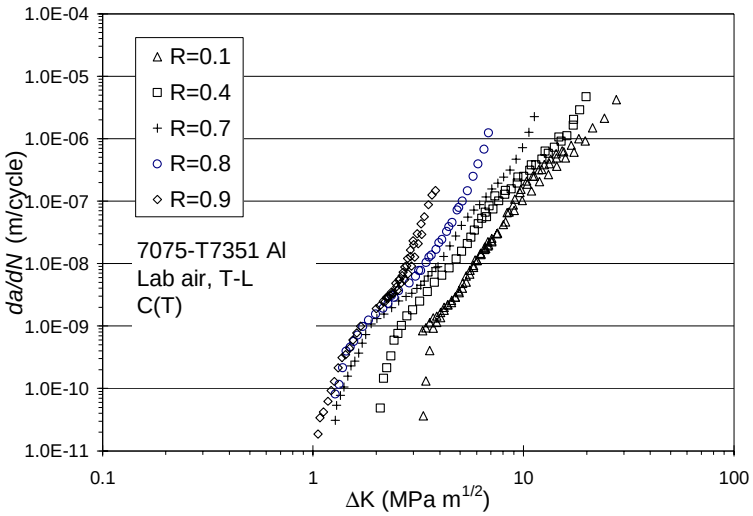

FIG. 14— *Constant R load reduction data*.

TABLE 1— *Threshold values using different precracking levels and test methods.*

R = 0.1

Specimen	Tension – K decreasing	Compression – K decreasing	Compression – K increasing
C(T)	2.30	N/A	1.49
GC(T)	1.37	1.46	N/A
M(T)	N/A	N/A	1.45

R = 0.7

Specimen	Tension – K decreasing	Compression – K decreasing	Compression – K increasing
C(T)	1.23	N/A	N/A
GC(T)	1.12	N/A	N/A
M(T)	N/A	N/A	1.05

Observations

It is apparent that the constant *R* load reduction procedure is producing ambiguous results in 7075-T7351 aluminum alloy for 12.7 mm thick specimens. First, the precracking level of the GC(T) data is studied to identify any effects of remote plasticity-induced crack closure. An odd "bounce" seen in the data at a ΔK of approximately 1.9 MPa $m^{1/2}$ (*i.e.* the crack growth rate decreased with decreasing ΔK, then increased with decreasing ΔK, then decreased with decreasing ΔK) could be a likely indicator of remote closure. The initial decrease in the crack growth rate (FIG. 10) may be attributable to remote plasticity-induced crack closure, which would cause crack retardation. As the specimen is continued to be cycled, the smashing of the crack faces at the point of remote

closure will eventually reduce the influence of the remote closure on the crack tip. As the influence of remote closure diminishes, the crack will accelerate, shown as the rise in the data presented in FIG. 10. Finally, the crack growth rate once again decreases with decreasing ΔK to a threshold value. Examining the data presented in FIG. 10, the specimen with the higher precracking load exhibited a greater shift in crack growth rate, *i.e.* a bigger bounce. This data supports the hypothesis that remote plasticity-induced closure is causing the bounce in the data because the greater the precracking level, the more likely remote plasticity-induced closure exists [19]. Finally, the compression precrack GC(T) data does not exhibit a "bounce" because it is a K increasing test. Remote plasticity-induced closure is not feasible in a compression precrack, K increasing test. Therefore, the constant R load reduction tests must be experiencing remote plasticity-induced crack closure.

Comparison of the C(T) to the GC(T) specimen data (FIG 10 and 11) illustrates the crack closure effect due to plane-stress zone at the specimen surface. The oxide buildup typically found in a C(T) specimen along the crack front (FIG. 15) was not evident in the GC(T) configuration (FIG. 16). It appears that since the plane-stress plastic zones along the crack surface close prior to the interior plane-strain zone, due to larger plastic deformation at the same K level (FIG. 7), that oxide is being trapped in the crack wake in the full thickness specimen causing closure. The GC(T) specimen has a nearly constant tri-axial stress state along the crack front [23], unlike a C(T) specimen, and therefore has less chance of trapping oxide debris in the specimen. Furthermore, there is little evidence of oxide-buildup along the crack face of the M(T) specimen (FIG. 17), which is also nearly plane-strain. These observations suggest that the plane stress zones along the specimen surface do not directly effect the test results, but are the enabling mechanism for the oxide to buildup at the crack front, enabling oxide-induced crack closure.

The GC(T) specimen is nearly plane-strain along the entire crack front, unlike the C(T) which is a mixture of plane stress/strain. Therefore, the GC(T) has a slightly higher crack growth rate along the entire range of ΔK compared to the C(T), as shown in FIG. 10. M(T) specimens are also nearly plane-strain, and the crack growth rate data presented in FIG. 11 shows good agreement between the GC(T) and M(T) data. However, near threshold, the compression precrack, constant ΔK data appears to be independent of specimen configuration. This would imply that as the plastic zone gets smaller, and there are no remote closure issues, there is no specimen configuration effect.

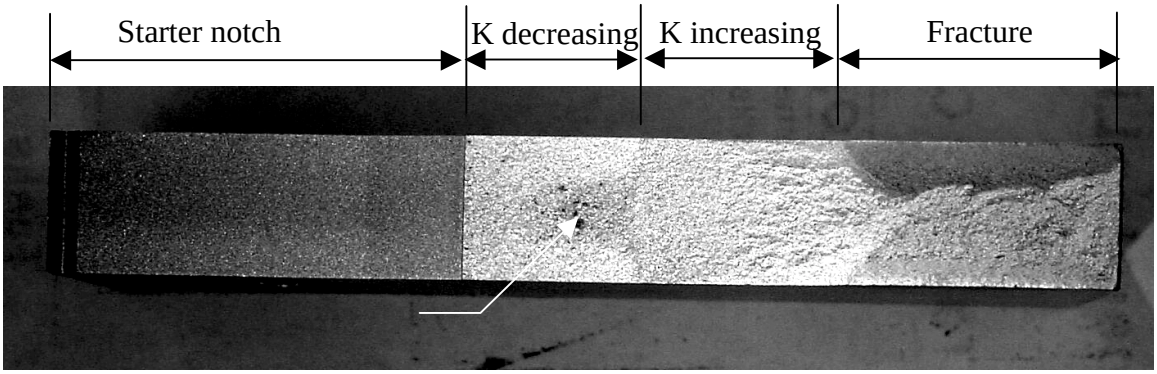

FIG. 15— *C(T) specimen fracture surface.*

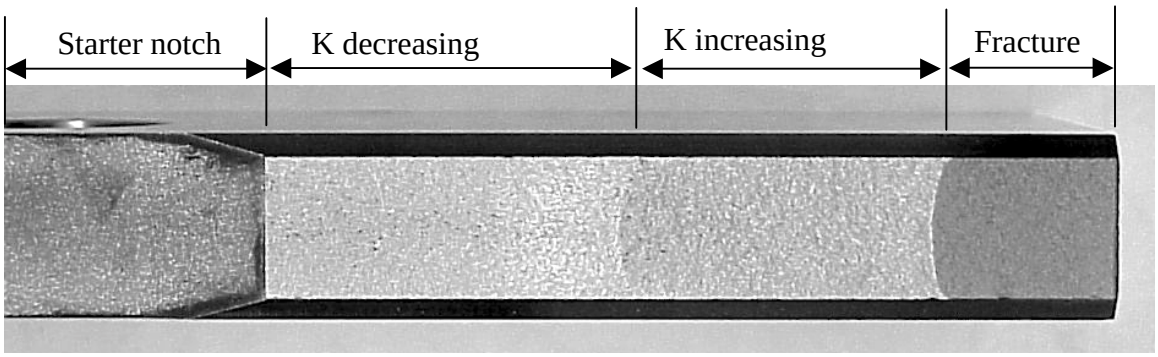

FIG. 16— *GC(T) specimen fracture surface.*

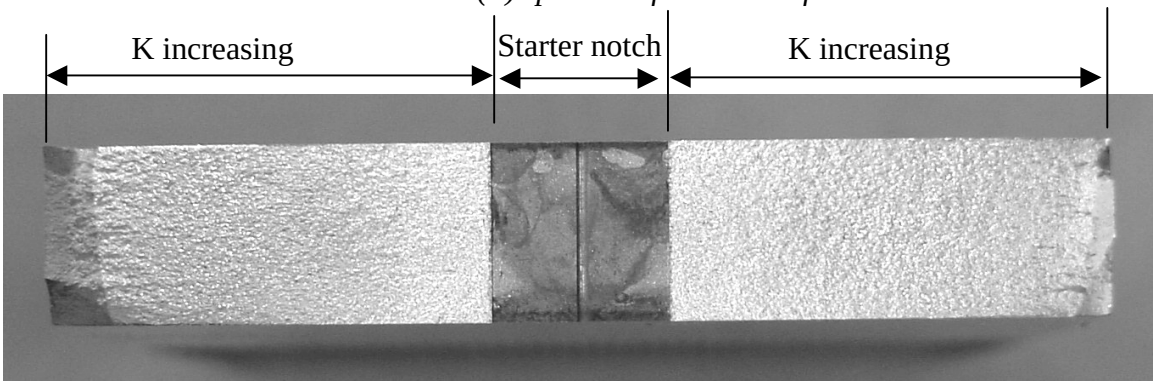

FIG. 17— *M(T) specimen fracture surface.*

Concluding remarks

The ASTM standard method E647, for producing fatigue crack growth thresholds produces artificially high values due to crack closure induced by the test procedure in 7075-T7351 aluminum alloy. The foundation for this argument is based upon plasticity theory and mechanics. It is important to note that these findings are based solely on testing in this material (7075 Al) and that continued research into the test methodologies and other materials will be required to make general conclusions. Constantly decreasing ΔK throughout a test will produce remote crack closure if the minimum loads are below the opening load. By implementing a compressive precracking scheme the effect of the residual plasticity at the notch is virtually eliminated. However, the constant *R* load reduction method still induces remote closure simply by initiating the test at a higher load than at the test conclusion. Conversely, the constant K_{max} load reduction method minimizes this effect by maintaining a high *R* load levels that keep the entire crack open. Utilizing middle through crack, M(T), and compact tension, C(T), specimens to produce K increasing data has illustrated that the fatigue crack growth threshold generated using the constant *R* load reduction method can be nonconservative by more than a factor of two (FIG. 11).

The constant *R* load reduction method also enables oxide-induced crack closure in 7075-T7351 aluminum alloy, due to plane stress plasticity at the specimen surface trapping oxide debris in the crack. Oxide-induced closure is not evident in K increasing tests because the crack-tip displacements are increasing throughout the test, precluding the development of oxide-induced closure.

The generation of fatigue crack growth thresholds for 7075-T7351 aluminum alloy has provided the foundation for further research. These new threshold test methods should be further developed and applied to other materials to generate new data sets with accurate threshold values. Future results may indicate that some materials exhibit little plastic deformation and therefore the current data set remains valid. However, it could be unconservative to assume that any data set is valid without a modicum of tests utilizing the new methods for verification.

It is the authors' goal to develop a fatigue crack growth threshold test method without load history effects due to remote plasticity-induced closure that can be conducted at a specified *R*. At this time, no current ASTM specified method can accomplish this. However, using compression-compression precracking and a K increasing test procedure will generate a fatigue crack growth curve from threshold to fracture at a specific *R* value without load history effects.

References

[1] Paris, P.C. and Erdogan, F., "A Critical Analysis of Crack Propagation Laws," Transactions of the ASME, Journal of Basic Engineering, Series D, 85, 3, 1963.

[2] Barsom, J.M., "Fatigue-Crack Propagation in Steels of Various Yield Strengths," *Transactions of the ASME, Journal of Engineering for Industry*, Series B, *93*, 4, November 1971.

[3] Frost, N.E., "The Growth of Fatigue Cracks," *Proceedings of the First International Conference on Fracture*, Sendai, Japan, 1966, pp. 1433.

[4] Bucci, R.J., "Development of a Proposed ASTM Standard Test Method for Near-Threshold Fatigue Crack Growth Rate Measurement" *Fatigue Crack Growth Measurement and Data Analysis, ASTM STP 738*, American Society for Testing and Materials, West Conshohocken, PA, 1981, pp. 5-28.

[5] "Damage Tolerance and Fatigue Evaluation of Structure", *Federal Aviation Regulations*, Title 14 Code of Federal Regulations, Part 25, Section 571.

[6] Engine Structural Integrity Program (ENSIP), MIL-STD-1783 (United States Air Force), 30, November 1984.

[7] Pearson, S., "Initiation of Fatigue Cracks in Commercial Aluminum Alloys and the Subsequent Propagation of Very Short Cracks," *Engineering Fracture Mechanics*, *7*, 2, 1975, pp. 235-247.

[8] Taylor, D. and Knott, J.F., "Fatigue Crack Propagation Behavior of Short Cracks – The Effects of Microstructure," *Fatigue of Engineering Materials and Structures*, *4*, 2, 1981, pp. 147-155.

[9] Taylor, D. and Knott, J.F., "Growth of Fatigue Cracks from Casting Defects in Nickel Aluminum Bronze," *Proceedings of the Metal Society Conference on Defects and Crack Initiation in Environment Sensitive Fracture*, University of Newcastle-on-Tyne, 1981.

[10] Smith, S.W. and Piascik, R.S., "An Indirect Technique for Determining Closure-Free Fatigue Crack Growth Behavior," *Fatigue Crack Growth Thresholds, Endurance Limits, and Design, ASTM STP 1372*, American Society for Testing and Materials, West Conshohocken, PA, 2000, pp. 109-122.

[11] Herman, W.A., Hertzberg, R.W. and Jaccard, R., "A Simplified Laboratory Approach for the Prediction of Short Crack Behavior in Engineering Structures," *Fatigue and Fracture of Engineering Materials and Structures*, *11*, 4, 1988, pp. 303-320.

[12] Hertzberg, R.W., Herman, W.A. and Ritchie, R.O., "Use of a Constant K_{max} Test Procedure to Predict Small Crack Growth Behavior in 2090-T8E41 Aluminum-Lithium Alloy," *Scripta Metallurgica*, *21*, 1987, pp. 1541-1546.

[13] Marci, G., "Fatigue Crack Propagation Threshold: What is it and How is it Measured?" *Journal of Testing and Evaluation*, JTEVA, *26*, 3, 1998, pp. 220-233.
[14] Haddad, M.H., Topper, T.H. and Smith, K.N., "Prediction of Non Propagating Cracks," *Engineering Fracture Mechanics, 11*, 3, 1979, pp. 573-584.
[15] Newman, Jr., J.C. and Piascik, R.S. (Eds.), *Fatigue Crack Growth Thresholds, Endurance Limits, and Design*, *ASTM STP 1372*, American Society for Testing and Materials, West Conshohocken, PA, 2000.
[16] Wu, X.J., Wallace, W. and Koul, A.K., "A New Approach to Fatigue Threshold", *Fatigue & Fracture of Engineering Materials & Structures, 18*, 7/8, 1995, pp. 833-845.
[17] Elber, W., "The Significance of Fatigue Crack Closure," *Damage Tolerance in Aircraft Structures, ASTM STP 486*, American Society for Testing and Materials, West Conshohocken, PA, 1971, pp. 230-242.
[18] Chen, D.L., Weiss, B. and Stickler, R., "Effect of Stress Ratio and Loading Condition on the Fatigue Threshold," *International Journal of Fatigue*, 14, 1992, pp. 325-329.
[19] Newman, Jr., J.C. and Elber, W. (Eds.), *Mechanics of Fatigue Crack Closure, ASTM STP 982*, American Society for Testing and Materials, West Conshohocken, PA, 1988.
[20] Forman, R.G., "Study of Fatigue-Crack Initiation from Flaws Using Fracture Mechanics Theory," *Air Force Flight Dynamics Laboratory Technical Report AFFDL-TR-68-100*, Wright-Patterson Air Force Base, Dayton, Ohio, Sept. 1968.
[21] Irwin, G.R., "Linear Fracture Mechanics, Fracture Transition, and Fracture Control," *Engineering Fracture Mechanics*, *1*, 2, Aug. 1968.
[22] McClintock, F.A. and Hult, J., "Elastic-Plastic Stress and Strain Distribution Around Sharp Notches in Repeated Shear," *Ninth International Congress on Applied Mechanics*, New York, 1956.
[23] Andrews, W.R. and Shih, C.F., "Thickness and side-groove effects on *J*- and δ-resistance curves for A533-B steel at 93^{o}C," *Elastic-Plastic Fracture, ASTM STP 668*, American Society for Testing and Materials, West Conshohocken, PA, 1979, pp. 426-450.
[24] Shih, C.F., deLorenzi, H.G. and Andrews, W.R., *International Journal of Fracture*, *13*, 1977, pp. 544-548.
[25] Topper, T.H. and Au, P., "Cyclic strain approach to fatigue in metals," *AGARD lecture series 118, Fatigue Test Methodology*, The Technical University of Denmark, Denmark, Oct. 19-20, 1981.
[26] Conle, A. and Topper, T.H., "Evaluation of small cycle omission criteria for shortening of fatigue service histories," *International Journal of Fatigue*, Jan. 1979.
[27] Pippan, R., Plochl, L., Klanner, F. and Stuwe, H.P., "The Use of Fatigue Specimens Precracked in Compression for Measuring Threshold Value and Crack Growth," *Journal of Testing and Evaluation*, JTEVA, Vol. 22, No. 2, 1994, pp. 98-103.
[28] Forth, S.C., Newman, J.C., Jr., and Forman, R.G., "On Generating Fatigue Crack Growth Thresholds," *International Journal of Fatigue*, Vol. 25, 2003, pp. 9-15.
[29] Shivakumar, K.N. and Newman, Jr., J.C., "Verification of Effective Thicknesses for Side-Grooved Compact Specimens," *Engineering Fracture Mechanics, 43*, 2, 1992, pp. 269-275.
[30] Newman, Jr., J.C., "Stress Analysis of the Compact Specimen Including the Effects of Pin Loading," *Fracture Analysis, ASTM STP 560*, American Society for Testing and Materials, West Conshohocken, PA, 1974, pp. 105-121.
[31] Feddersen, C.E., "Discussion of Plane-Strain Crack Toughness Testing of Metallic Materials," *Current Status of Plane Strain Crack Toughness Testing of High-*

Strength Metallic Materials, ASTM STP 410, American Society for Testing and Materials, West Conshohocken, PA, 1967, pp. 77-79.
[32] Hudak, Jr., S.J., Saxena, S.J., Bucci, A. and Malcolm, R.C., "Development of Standard Methods of Testing and Analyzing Fatigue Crack Growth Rate Data – Final Report," *AFML TR 78-40*, Air Force Materials Laboratory, Wright Patterson Air Force Base, OH, 1978.
[33] Saxena, A., Hudak, Jr., S.J., Donald, J.K. and Schmidt, D.W., "Computer-Controlled Decreasing Stress Intensity Technique for Low Rate Fatigue Crack Growth Testing," *Journal of Testing and Evaluation*, *8*, 1, 1980, pp. 19-24.
[34] Au, P., Topper, T.H. and El Haddad, M.L., "The Effects of Compressive Overloads on the Threshold Stress Intensity for Short Cracks," *Behavior of Short Cracks in Airframe Components, AGARD Conference Proceedings No. 328*, pp. 11-1 - 11-7.
[35] Newman, Jr., J.C., "An Evaluation of the Plasticity-Induced Crack Closure Concept and Measurement Methods," *ASTM STP-1343*, American Society for Testing and Materials, West Conshohocken, PA, 1999, pp. 128-144.
[36] James, M. A., Forth, S. C., and Newman, J. A., "Load History Effects Resulting from Compression Precracking," *Fatigue and Fracture Mechanics: 34th Volume, ASTM 1461*, S. R. Daniewicz, J. C. Newman, Jr., and K.-H. Schwalbe, Eds., ASTM International, West Conshohocken, PA, 2004.
[37] NASGRO Material Database, www.nasgro.swri.org, 2004.